

# Preliminary shielding analysis for the CSNS target station monolith<sup>\*</sup>

ZHANG Bin(张斌)<sup>1;1)</sup> CHEN Yi-Xue(陈义学)<sup>1;2)</sup> YANG Shou-Hai(杨寿海)<sup>1</sup> WU Jun(吴军)<sup>1</sup>  
YIN Wen(殷雯)<sup>2</sup> LIANG Tian-Jiao(梁天骄)<sup>2</sup> JIA Xue-Jun(贾学军)<sup>2</sup>

<sup>1</sup> North China Electric Power University, School of Nuclear Science and Engineering, Beijing 102206, China

<sup>2</sup> Institute of Physics, Chinese Academy of Sciences, Beijing 100190, China

**Abstract** The construction of the China Spallation Neutron Source (CSNS) has been initiated at Dongguan, Guangdong, China. In spallation neutron sources the target station monolith is contaminated by a large number of fast neutrons whose energies can be as large as those of the protons of the proton beam directed towards the tungsten target. A detailed radiation transport analysis of the target station monolith is important for the construction of the CSNS. The analysis is performed using the coupled Monte Carlo and multi-dimensional discrete ordinates method. Successful elimination of the primary ray effects via the two-dimensional uncollided flux and first collision source methodology is also illustrated. The dose at the edge of the monolith is calculated. The results demonstrate that the doses received by the hall staff members are below the required standard limit.

**Key words** shielding, CSNS, neutron transport

**PACS** 28.41.Qb, 28.20.Gd

## 1 Introduction

The China Spallation Neutron Source (CSNS) [1, 2] complex is designed to provide multidisciplinary platforms for scientific research and applications for national institutions, universities and industries. Spallation, the process in which a heavy nucleus emits a large number of nucleons as a result of being hit by a high-energy particle, thus greatly reducing its atomic weight, has become an important technique for the production of high-intensity neutron fluxes.

The CSNS target station has the basic function of converting the short pulse, high-average-power, 1.6 GeV, proton beam into 18 lower-energy, short-pulsed neutron beams, which can provide the required neutrons for neutron scattering instruments. Tungsten is a proven target material for the CSNS design beam power. A tantalum cladding is adopted to deal with the issue of material brittleness caused by radiation damage and the corrosion caused by the heavy

water coolant. The position of the target is within a layered steel and concrete shield monolith which is approximately 12 meters in diameter.

A methodology of coupled Monte Carlo and multi-dimensional discrete ordinates methods has been implemented to perform the shielding analyses [3–5]. It is expected that careful design analyses will bring an optimal layout of the shielding layers and the instrumentation around the target–moderator–reflector complex (TMRC).

## 2 Methodology and cross section library

The radiation transport analyses are performed to characterize the streaming through the CSNS target station monolith using DORT [6], a two-dimensional discrete ordinates neutron/photon transport code. Initially, MCNPX [7] is used to calculate a source sur-

---

Received 15 December 2009

<sup>\*</sup> Supported by National Natural Science Foundation of China (10875042, 10705011), Program for Changjiang Scholars and Innovative Research Team in University (IRT0720) and Beijing Science New Star Plan Project (2007B058)

1) E-mail: rnzhangbin@163.com

2) E-mail: yxchen@ncepu.edu.cn

©2010 Chinese Physical Society and the Institute of High Energy Physics of the Chinese Academy of Sciences and the Institute of Modern Physics of the Chinese Academy of Sciences and IOP Publishing Ltd

rounding the CSNS target, moderators and reflector. This source is used as the initial source in this analysis. Next, considering that this model contains some large void regions, thus is susceptible to ray effects, this analysis emphasizes that ray effects should be eliminated. Ray effects are a consequence of the discrete ordinates approximation of the angular dependence in the transport equation and typically characterize the transport of neutral particles in air and weakly scattering materials. The easiest way to overcome this difficulty is to raise the order of the angular quadrature. However, in this problem this way can result in a significant increase in computation time due to the large physical size of the monolith. Another way to deal with such effects is to divide the calculation into three stages. First, the GRTUNCL [8] code is executed to produce the first collision source and uncollided flux distributions throughout the model. Second, the first collision source is used to drive a DORT calculation to yield the fully collided group flux spatial distribution. Finally, the uncollided and fully collided group flux distributions are added together, and then the sum is folded with the flux to dose conversion factors to obtain the total dose field distribution.

Figure 1 is a flow chart of this calculation sequence. The code NJOY [9] is used to produce a multi-group set library. The code TRANSX is used to pre-treat the MATXS file to a simple library which can be used by Sn codes, such as ANISN or DORT. The flow chart includes both the cross section library production and the radiation transport calculation.

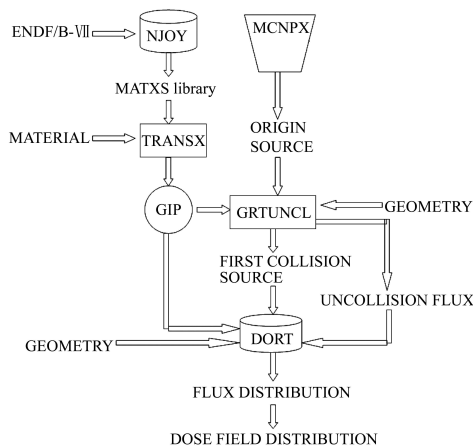


Fig. 1. Calculation flow diagram for the monolith analyses.

All of these DORT and GRTUNCL calculations use the newly developed 150 MeV cross-section li-

brary HEST1.0<sup>1)</sup>. The library HEST1.0 contains 81 high-energy neutron groups, 172 low-energy neutron groups and 48 photon groups. The library contains nuclides which included 99.6% nucleus density in high density concrete. The library also includes all the nuclides except manganese in materials such as low carbon steel and stainless steel 316.

### 3 Geometric model and source term

The CSNS target monolith is the primary structure that contains the TMRC and the shutters. Outside the reflector plug assemblies is the bulk shield, comprised of low carbon steel, which is surrounded by a high-density concrete biological shield. The model doesn't include some details present in the actual facility. Regions of similar materials are combined and considered as homogenous mixtures. As typical shielding materials, high density concrete and low carbon steel are selected. Fig. 2 shows some of the material zones and components of the CSNS target monolith.

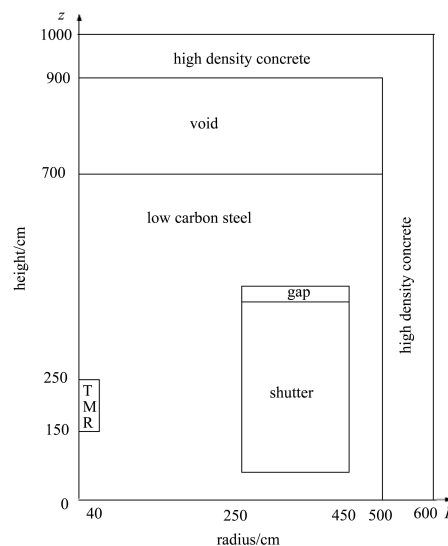


Fig. 2. CSNS monolith model.

The target station monolith is cylindrical in shape with the target located at the center of the monolith and 200 cm above the bottom. The proton beam line enters the target monolith horizontally and 18 neutron beam lines penetrate radially outward from the target. The CSNS shutters are positioned on each neutron beam line approximately 250 cm out from the target in the steel region, and stand parallel to the axis of the target monolith. The shutters move in the axial direction to open and close.

1) WU J, CHEN Y X, ZHANG B, et al. High Energy Multi-group Library HEST1.0 based on ENDF/B-VII: Development, Verification and Application to the CSNS Shielding Design

The TMRC consists of a Tungsten target, a stainless steel target container, and a number of moderators. They are all incased by a cooled reflector. MCNPX calculates the source of the secondary particles and their energy spectra as they are leaking through the TMRC surface. At the same time, a simple cylindrical model describing the gross features of the TMRC is developed. Fig. 3 presents the energy spectrum of the neutrons leaking through the TMRC cylindrical surface in this analysis.

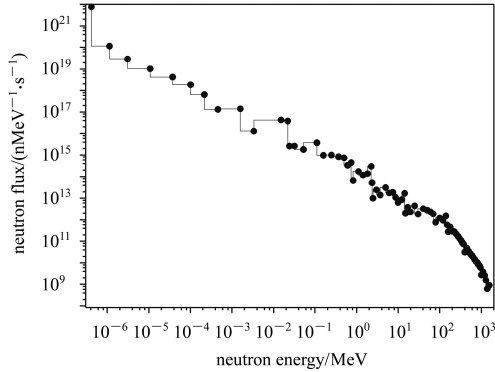


Fig. 3. The energy spectrum of the neutrons leaking through the TMRC cylindrical surface.

## 4 Shielding analysis

It is a difficult task to accomplish the deep penetration calculations with reasonable accuracy for the CSNS shielding design. The shielding calculation is a coupled neutron and photon transport calculation. The purpose of this work is to evaluate the biological shield design of the CSNS target station, in order to make sure that the dose outside the shield's surface meets the radiation criteria under normal operational conditions. The biological shield typically consists of multi-layers combination of iron and concrete. Different shielding configurations of the target station are calculated and discussed. The first model consists of a 550 cm thick steel layer and a 50 cm thick concrete layer. The second one consists of a 500 cm thick steel shield and a 100 cm thick concrete layer. The third one consists of a 450 cm thick steel shield and a 150 cm thick concrete layer. As a last one,

we evaluate the following sandwich configuration: a 400 cm thick steel layer covered by 50 cm thick concrete then a 100 cm thick steel layer and the outer concrete layer with a thickness of 50 cm.

Figure 4 presents the results of the DORT calculation for the energy distribution of the neutron flux densities. The figure clearly shows the attenuation of the neutron spectra with increasing shield thickness and that the major energy part shifts towards the low-energy region mainly due to elastic scattering. The influence of the concrete component in absorbing low-energy neutrons is also depicted in Fig. 4. The spectrum at 550 cm is already close to a  $1/E$  distribution.

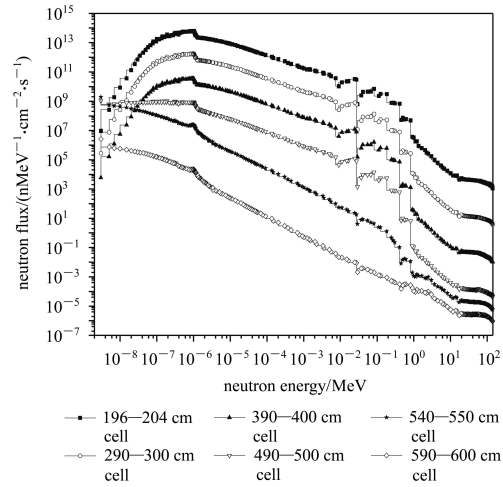


Fig. 4. Neutron flux density energy spectra for model 2.

Neutron and photon dose equivalent rates have been calculated by folding the local neutron and photon flux with the appropriate flux to dose equivalent conversion factors. The neutron and photon dose conversion factors are based on the ICRP74 recommendations. The biggest dose equivalent rates for each model surface are presented in Table 1 and usually occur at the monolith surface of the level with a gap.

In general, the neutron dose decreases exponentially with increasing thickness of the iron layer. In the low energy region the concrete has a better shielding performance than the iron due to the elastic scattering effect of hydrogen contained in the concrete. Therefore, the outer concrete layer reduces the dose

Table 1. The biggest dose rate for various shield configurations.

shield configuration	total dose rate/( $\mu\text{Sv/h}$ )	neutron dose rate/( $\mu\text{Sv/h}$ )	photon dose rate/( $\mu\text{Sv/h}$ )
Model 1	1.33E+00	4.47E-01	8.85E-01
Model 2	6.45E-02	4.95E-03	5.96E-02
Model 3	9.97E-03	9.27E-03	6.98E-04
Model 4	7.98E-01	2.61E-01	5.36E-01

rate quite effectively. Along with the increase in the concrete thickness goes an increasing high-energy neutron dose, thus demonstrating the liability of model 3 in shielding high-energy neutrons. The characteristics in Fig. 5 are obvious. Finally, it is evident from our calculation that a sandwich structure is an economical choice. All models satisfy the required criterion of a dose equivalent rate less than  $2.5 \mu\text{Sv/h}$ .

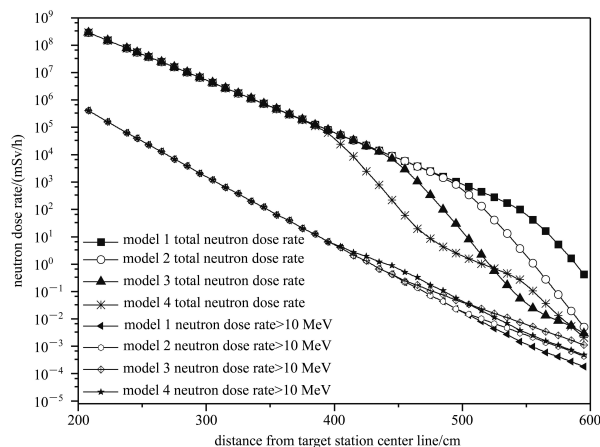


Fig. 5. Attenuation of neutron dose for various shield configurations.

The analysis of the streaming through the CSNS shutter travel gap is a parametric study. A position for the gap has been set, but we are interested in knowing if it could be moved closer to the neutron beam line. So the shutter becomes smaller and accordingly the weigh and cost of building and maintaining will be less. The gap is simulated as a continuous ring in the target monolith, which makes the modeling a conservative one. This calculation is used to determine the configuration and position of the shutter travel gap. The goal for the shutter travel gap analysis is to have the dose anywhere along the edge of the concrete collar less than  $2.5 \mu\text{Sv/h}$ . In this study, the gap was located at 5 different positions. Table 2 lists the results of this parametric study. It is obvious that as the travel gap is moved to a lower

position, the dose increases due to the more intense radiation fields.

Table 2. Results of “Top Gap” parametric study.

height of the shutter/cm	gap centerline dose/ $(\mu\text{Sv/h})$
500	$7.46 \times 10^{-3}$
470	$1.81 \times 10^{-2}$
450	$3.18 \times 10^{-2}$
420	$7.59 \times 10^{-2}$
400	$1.27 \times 10^{-1}$

The influence of the shutter step gap on radiation shielding is also analyzed. The step gap inside is taller than that outside. It is modeled as a continuous ring extending over 360 degrees around the target monolith. This approximation will result in conservatively high doses. From the calculation result it is obvious that the step gap can reduce the peak dose along the edge of the concrete collar by about 60.4% compared with the solid gap at the edge of the concrete collar.

## 5 Conclusion

A deep-penetration calculation is performed with the two-dimensional discrete ordinates method DORT code. The neutron energy spectra behind a very thick shield of approximately 5-m-thick low carbon steel and 1-m-thick high density concrete are calculated in the energy range from thermal to 150 MeV. Besides the long computational time and the complicated geometry of the model, the greatest difficulty is the occurrence of ray effects. We succeeded in eliminating ray effects by the proper use of the code GRTUNCL2D. A preferable shielding model has been obtained in the calculation and the dose along the edge of the concrete collar received by the hall staff members are below the required standard limit.

*The authors would like to thank Chinese Academy of Sciences for the work they did running MCNPX to help create our sources, and their guidance.*

## References

- FANG S X, FU S N, QIN Q et al. Journal of the Korean Physical Society, 2006, **48**(4): 697–702
- WEI J, CHEN H S, CHEN Y W et al. Nuclear Instruments and Methods in Physics Research A, 2009, **600**: 10–13
- Miller T M. Oak Ridge National Laboratory, 2001, 106100200-DA0001-R00
- Nakaoa N, Nunomiya T, Iwase H et al. Nuclear Instruments and Methods in Physics Research A, 2004, **530**: 379–390
- Koprivnikar I, Schachinger E. Nuclear Instruments and Methods in Physics Research A, 2002, **487**: 571–584
- Rhoades W A, Childs R L. Oak Ridge National Laboratory, 1992, ORNL/TM-11778
- Hughs H G, Prael R E, Little R C. Los Alamos National Laboratory, 1997
- Childs R L. Oak Ridge National Laboratory, 1996, CCC-6501DOORS3.2
- MacFarlane R E, Muir D W. Los Alamos National Laboratory, 1994, Tech. Rep. LA-12740-M